

Open Space Diffusive Filter for Simultaneous Species Retrieval and Separation

Prerit Mathur, Anna Fomitcheva Khartchenko, Andrew J. deMello,* and Govind V. Kaigala*

Cite This: *Anal. Chem.* 2020, 92, 11548–11552

Read Online

ACCESS |



Metrics & More

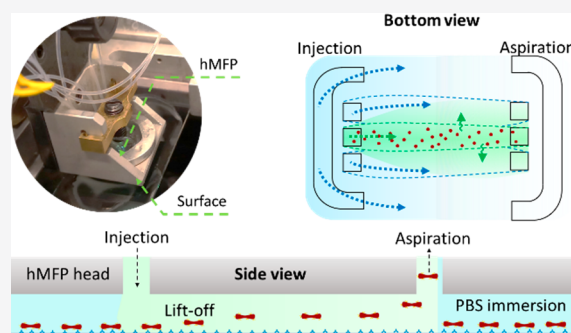


Article Recommendations



Supporting Information

ABSTRACT: We present a novel method for the local retrieval of surface bound species and their rapid in-line separation using an open space microfluidic device. Separation can be performed in less than 30 s using the difference in diffusivities within parallel microfluidic flows. As a proof-of-principle, we report the rapid and efficient filtration of polystyrene beads from small molecules and surface bound red blood cells from dimethyl sulfoxide for antigen typing.



The separation of analytes from heterogeneous mixtures is central to numerous diagnostic tests and biological workflows. Microfluidic flows have been shown to provide a robust way to separate microscale species through manipulation of small fluid volumes and flow paths.¹ The basic idea of using an external force field orthogonal to a flow to affect separation was popularized by Giddings in 1976 in his seminal work on flow field-flow fractionation.² Such a transverse force was shown to be effective at separating solute species based on the balance of the strength of their interaction with this external field and diffusion. In the intervening years several flow-based separation modes have been proposed, leveraging differences in density, deformability, solvent affinity, mobility, or size.¹ Size has been widely used to separate species in flow, using chromatographic interactions³ or micropillars.⁴ Interestingly, obstacle-free methods (which do not suffer from clogging or fouling of the separating media) are amenable to continuous flow operation and may utilize nonuniform flow profiles,⁵ non-Newtonian fluids⁶ or simply differences in species diffusivity.

Diffusive separation can be performed by using wide bore hydrodynamic chromatography⁷ (leveraging difference in diffusivities and parabolic flows to separate species), bidirectional flow filtration⁸ (which uses electroosmotic flow to manipulate streams in an antiparallel fashion), and H-filters⁹ (which use closed microfluidic channels to separate species of differing diffusivity in two adjacent parallel flows). A variation of this device, the T-sensor,¹⁰ has also been used to measure the diffusivity of solute species. Both of these functionalities have recently been transferred to paper-based flow networks.¹¹ Although numerous applications of these devices have been demonstrated,^{12–15} a major limitation of closed microfluidic systems is a lack of access to the surface, which significantly

reduces applicability to biological substrates and surface bound species.

Open space microfluidics is an emerging class of the technology set in which at least one boundary confining the fluid flow of a system is removed, exposing the fluid to the atmosphere or another interface such as a second fluid. In such a modality solid physical walls are replaced by dynamic flowing walls that are able to confine an analyte of interest. While several techniques, including dip pen nanolithography¹⁶ and atomic force microscopy,¹⁷ permit access to a surface and allow the retrieval of species of interest, surface access in flowing environments can be achieved using the microfluidic probe (MFP). With an MFP, the liquid is injected onto a surface and aspirated from a neighboring aperture, thus creating hydrodynamic confinement, the shape of which can be changed depending on the placement of apertures within the MFP.¹⁸ The MFP can be moved over centimeter-scale regions to sample areas of interest, with the fluid dynamically interacting with surface-associated species on micron length scales. It has been shown to be highly efficient at depositing analytes on a biological surface and removing surface adhered nucleic acids¹⁸ and cells.¹⁹ These retrieved species, when put through workflows that involve multistep processes, are typically subject to sample loss.²⁰ Accordingly, the integration of a separation step with retrieval would reduce losses and even

Received: May 20, 2020

Accepted: July 8, 2020

Published: July 8, 2020



allow for the analysis of rare species. Furthermore, time of contact of surface adhered species with the retrieval solution would be reduced.

OPERATING PRINCIPLE

Here, we present a microfluidic tool that combines the retrieval and separation of species with open space microfluidics for the filtration of chemical and biological species based on their diffusivities, the open space diffusive filter. Specifically, we use a horizontally oriented microfluidic probe (hMFP) to establish three parallel open space flow streams. Lower diffusivity species remain in the central stream, while higher diffusivity solutes “spread out” evenly across all the streams, thus separating the two components. To demonstrate the efficacy of our method, we present the separation of microbeads and dye molecules in flow and measure the diffusivity of fluorescein. Furthermore, we report the single-step removal of cells bound to a surface using a harsh chemical stimulus, which is simultaneously removed to enhance cell viability for further downstream analysis.

We leverage the diffusive boundary between parallel flows established on the scanning microfluidic device. In such an open space system, advection and diffusion are the two primary processes involved in species transport. To ensure separation of a mixture of two species, the diffusive spread of the first species must dominate the advective motion of the other. Accordingly, the behavior of the species in the flows can be described by two time scales.²¹ The diffusion time scale, τ_{diff} is given by

$$\tau_{\text{diff}} = \frac{w^2}{D} \quad (1)$$

and defines the time required for a species to diffuse across the channel width. Similarly, the advection time scale, τ_{adv} is given by

$$\tau_{\text{adv}} = \frac{L}{v_0} \quad (2)$$

and describes the average time it takes for a species to travel from the inlet to the outlet. Here, L and w are the open channel length and width, respectively, v_0 is the characteristic flow velocity, and D is the diffusivity of the species. A mixture of two species can be separated into components by passive diffusion alone in the microchannel, if species 1 diffuses across the channel width, whereas species 2 does not diffuse appreciably. Accordingly, for species 1, $\tau_{\text{diff},1} \ll \tau_{\text{adv},1}$ and for species 2, $\tau_{\text{diff},2} \geq \tau_{\text{adv},2}$. For the rapidly diffusing species 1, the limiting value of diffusivity (D_1^*) for separation can be found by equating, $\tau_{\text{diff}} = \tau_{\text{adv}}$, that is

$$D_1^* = \frac{v_0 w^2}{L} \quad (3)$$

Eq 3 predicts a separation length of approximately 1 mm that is needed for a small molecule ($D \sim 10^{-10} \text{ m}^2/\text{s}$) to diffuse across the channel width at a low flow rate (30 nL/min) (Figure S1, Supporting Information Note 3). Since diffusion is responsible for transport of species transverse to the flow stream, a parallel flow system can also be used to measure the diffusivity. The solution of the advection-diffusion equation adapted for parallel flow is given by

$$C(x, y) = \frac{C_0}{2} \left[1 - \operatorname{erf} \left(\frac{y}{2\sqrt{Dx/U}} \right) \right] \quad (4)$$

where C is the concentration of a species with diffusivity D at location (x, y) for a flow with an average velocity U and C_0 is the injected dye concentration.²²

To demonstrate the functionality of species separation in open space, we designed a scanning hMFP able to establish adjacent parallel flows (on a surface) that stay confined in their respective flow paths. One central stream and two side streams were used to collect the rapidly diffusing solute from both sides of the central stream (Figure 1). This arrangement provided an

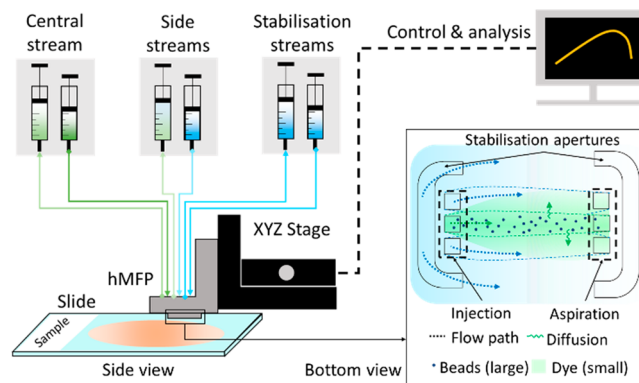


Figure 1. Schematic of the experimental setup illustrating the open space scanning a surface sample. Inset shows principle of the diffusive separation process in parallel flows generated by the microfluidic probe.

added advantage of greater diffusive separation of the solute (i.e., 1/3 of the initial amount as compared to 1/2 for two streams). To ensure that the flow remained confined along the entire path length, stabilization apertures were added to the design. These ensured the creation of a complete sheath flow and helped maintain a low ratio of aspiration to injection flow rates to conserve the parallel profiles (Figure S4).

EXPERIMENTAL SECTION

Horizontal Microfluidic Probe (MFP) Design. The horizontal microfluidic probe (hMFP) consists of a 4-in. double-side polished silicon wafer (Si-Mat, Germany) that is 500 μm thick and bonded to a plain glass wafer (Plan Optik AG, Germany) also 500 μm thick. All manufacturing steps were performed in-house at either the Binnig and Rohrer Nanotechnology Center (BRNC, ETH Zürich) or a standard laboratory. Briefly, the hMFP design is etched into a silicon wafer, with corresponding access holes drilled through the glass wafer. Both substrates are then aligned and joined using anodic bonding. Finally, the individual hMFP heads are diced, and the edges polished for use (Figure S2). Each hMFP head contains three 100 $\mu\text{m} \times 100 \mu\text{m}$ injection and aspiration apertures with an interaperture spacing of 50 μm . The distance between apertures is 1 mm. Stabilization apertures are also 100 μm in width, with a length of 800 μm for injection stabilization and 1000 μm for aspiration stabilization. A hMFP to surface distance of 100 μm was chosen (Supplementary Note 3).

Microfluidic Parallel Flow Setup. Prior to experiment, the hMFP was sonicated in a 1:1 mixture of ethanol and isopropanol for 5 min. The hMFP head was then inserted into a custom-built holder and held in place using a bespoke

PMMA and PDMS adapter, which also was used to guide the tubing (1/32 in.) toward the vias. The flows were controlled by six Nemesys syringe pumps from (Cetoni GmbH, Germany) (Figure S3). To establish parallel flows, sample injection was performed at 1 $\mu\text{L}/\text{min}$ for all streams, with an aspiration flow rate 1.5 $\mu\text{L}/\text{min}$ for all streams. Stabilization injection was performed at 10 $\mu\text{L}/\text{min}$ and stabilization aspiration at 8 $\mu\text{L}/\text{min}$ (Figure 2c).

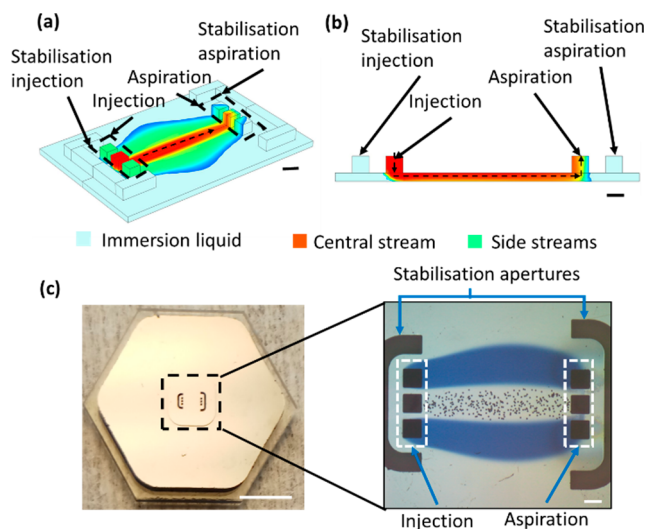


Figure 2. Implementation of open space diffusive separation using a microfluidic probe head. CFD simulations report the flow profiles in (a) the top and (b) side projections. Distinct colors represent different fluids in the central and side streams and the immersion liquid. (c) Image of the fabricated microfluidic device (bottom view, scale bar 2 mm) and the generated flow streams (scale bar 100 μm). The central flow is seeded with polystyrene beads and the side flow with blue dye.

For in-flow separation, the sample injection flow rate was set to 30 nL/min for all the streams and 50 nL/min for all sample aspiration streams (Figure 3a). Stabilization injection was done at 500 nL/min and stabilization aspiration at 300 nL/min. Fluorescein (Sigma-Aldrich Chemie GmbH, Switzerland) was used as a 100 μM solution in deionized water. For flow tracing, 8 μm Duke Standards polystyrene microspheres from (ThermoFisher, USA) were obtained as an aqueous solution with 0.3% solid content. This stock solution was diluted 20 times prior to use. A 0.4% stock solution of Trypan blue (Sigma-Aldrich Chemie GmbH, Switzerland) was also used as a flow tracer in selected experiments.

For on-surface RBC separation, a glass slide (ThermoFisher, USA) was coated with human IgG. Specifically, 200 μL of a 50 $\mu\text{g}/\text{mL}$ solution of human IgG (abcam, Germany) was deposited on the slide surface and left to incubate in the dark for 1 h. The slide was then washed with 500 μL of phosphate buffered saline (PBS) twice to remove any nonspecifically bound antibodies. 500 μL of 1% BSA in PBS buffer was then deposited on the surface to block any unbound sites and allowed to incubate in the dark for 1 h. Again, the surface was washed with 500 μL of PBS twice to remove any nonspecifically bound molecules. Finally, antihuman IgG coated RBCs (Immunocor Inc., USA) were deposited on the slide and left to incubate for 1 h. After washing twice with 500 μL of PBS, the slides were used immediately. For retrieval and separation experiments, a 50 nL/min flow rate was used for all

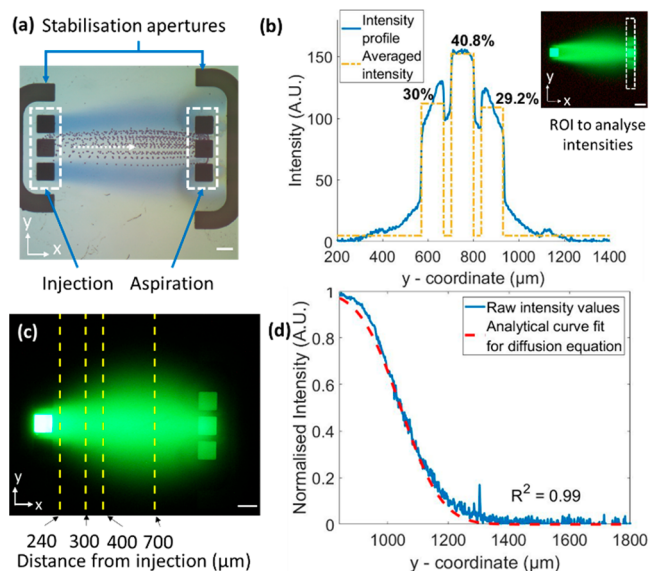


Figure 3. (a) Image stack reporting the aspiration of PS beads in the central stream and the blue tracer in the side streams. (b) Intensity profile of fluorescein dye at the aspiration channels calculated for the region of interest (ROI) shown in the inset. (c) Experimental locations for diffusivity measurements. (d) Analytical curve fit to calculate diffusivity. All scale bars are 100 μm .

sample injection streams and 80 nL/min for all aspiration streams. Stabilization injection was performed at 800 nL/min and stabilization aspiration at 500 nL/min.

Imaging Setup. Images were captured with a Nikon Ti-E epifluorescence microscope with a Mira (Lumencor Inc., USA) white light source and appropriate filter cubes (for FITC and brightfield measurements). A Nikon DS-Fi2 camera controlled by Nikon NIS software was used for imaging. Quantities of aspirated dye in each aspiration aperture were calculated through image analysis of fluorescence using a custom MATLAB script. The average intensity at each exit aperture was taken as a measure of the amount of aspirated dye. This intensity was normalized and fitted to eq 4 to extract diffusivities.

RESULTS AND DISCUSSION

To realize appropriate geometrical and flow parameters that sustain the flow profile, the aperture geometry and flow rates were calculated using finite element simulations in COMSOL. Parameters were chosen such that the central and side streams remained confined between the injection and aspiration apertures with minimal dilution, and stabilization apertures allowed surface access for the central flow streams (Figure 2a and b). The fabricated hMFP heads were then used to establish flows (Figure 2c) with tracers in the three streams. A relatively high flow rate ensured minimal diffusion for better visualization. As expected, the parallel flows remained confined and stable over extended periods of time.

Once stable parallel flows were established, differences in diffusivities were used to separate species in-flow in open space, in a manner analogous to a conventional H-filter. Initially, a mixture of a fluorescent dye (fluorescein) and 8 μm polystyrene (PS) beads was injected through the central injection channel. The confinement length for effective diffusive separation was calculated to be approximately 1 mm (Supplementary Note 3). Significantly, all PS beads were

aspirated from the central aperture owing to their low diffusivity (Figure 3a), while dye molecules diffused to the side streams and were aspirated through all the exit apertures (Figure 3b). In addition, the normalized intensity in the side channels was 59.2%, which is close to the theoretical maximum of 66% (assuming uniform diffusion across all exit channels). Device reliability was further judged from multiple experimental runs (Supplementary Note 4). In this regard, species with larger diffusion coefficients or a device with longer interaperture distances would generate a side channel aspiration closer to the theoretical maximum.

The parallel flow profile was then used to extract diffusivity values based on the theoretical model provided in eq 4. The fluorescence intensity across fluid streams was measured at multiple locations downstream of the injection aperture. Based on fits to the normalized intensity values at these different locations, the diffusivity of fluorescein was calculated to be $4.37 \pm 0.37 \times 10^{-10} \text{ m}^2/\text{s}$ (Supplementary Note 5), a value in good agreement previously reported measurements.²³

We developed the separation process further by leveraging inherent advantages of open space microfluidic flows to selectively access surface bound species. The ability to access surfaces can be helpful for a wide range of biological assays.²⁴ To prove principle, we present the simultaneous retrieval of species from a surface and their subsequent in-line separation. Such a workflow is of wide utility, for example in immunoassays using surfaces to bind ligands. One such assay is the antigen typing test, which is used to analyze the presence of user-defined antigens on the surface of red blood cells (RBCs) and which has recently been implemented as a microarray system.^{25,26} Here, antibodies are used to detect RBCs with the proteomic footprint of interest via hemagglutination or specific binding to a slide surface. In many situations, the RBC sample will be limited, with additional tests on “bound” RBCs being required, for instance, to test for anemia or microvascular perfusion^{27,28} after removal from the surface. Unfortunately, solvents commonly used to release bound RBCs are often incompatible with cell viability.²⁹ Accordingly, to ensure sample viability, solvent must be removed or diluted promptly after release is complete.

Specifically, we bound IgG modified RBCs to an antibody-coated glass slide (Figure 4a). We then injected a solution of

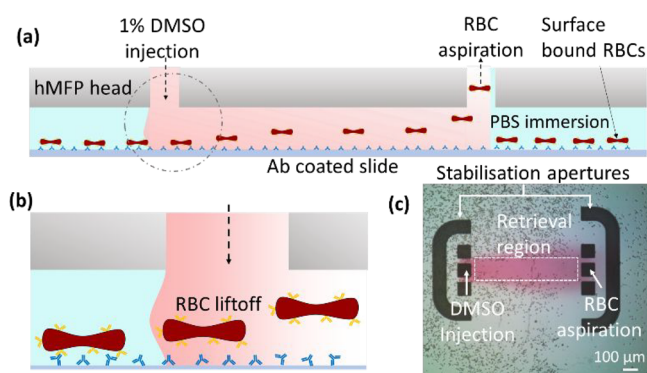


Figure 4. (a) Schematic of surface retrieval and diffusive separation. (b) Enlarged view detailing the RBC lift-off process. (c) RBCs are aspirated in the central channel, while DMSO is diluted by diffusion. The retrieval region is evidenced by an absence of RBCs and marked by the dotted rectangle. Every black speck seen on the surface is a RBC.

1% DMSO in deionized water to disrupt binding and cause the RBCs to “lift-off” in flow (Figure 4b). Since RBCs are large ($\sim 10 \mu\text{m}$ in diameter) and hence low in diffusivity, they remain in the central stream and are aspirated through the central exit channel for retrieval (Video S1). DMSO, being a small molecule, has a much higher diffusivity (approximately $10^{-9} \text{ m}^2/\text{s}$) and thus diffuses through all exits (Figure 4c). This translates to a DMSO concentration of approximately 0.4% with the aspirated RBCs in the central channel. Since higher DMSO concentrations are correlated with increased rates of RBC hemolysis,³⁰ such a diffusion-based separation process ensures that RBCs remain intact and have lower DMSO exposure. We found RBCs to remain visibly intact up to 20 min after in-line separation had been performed. It should be noted that in the present scenario, volumetric flow rates are in the nL/min range and thus will generate a negligible surface shear. This is supported by the fact that cells are not picked up by either the side or stabilization flows. The use of higher flow rates (e.g., Figure S4b) would also lead to RBC collection but with significantly reduced cell viability.³¹

CONCLUSION

We have presented an open space diffusive filter using a horizontal microfluidic probe. Unlike conventional closed microfluidic systems, the hMFP provides localized and controlled surface access, while low volumetric flow rates avoid the generation of excessive amounts of shear. Initial experiments, aimed at isolating PS beads from a fluorescein/bead mixture, demonstrated a filtration of 59.2% of the dye (compared to a theoretical limit of 66%) with a negligible loss of beads. Moreover, the platform was used for the efficient surface retrieval and in-line separation of RBCs from DMSO. It should be noted that the single pass filtration efficiency is limited by diffusion to 33% separation. However, simple recirculation of the flow allows efficiency enhancements of 33% for each recirculation pass, resulting in outstanding levels of purity when required. We envision the basic method to be particularly advantageous for surface retrieval and in-line separation processes. For example, rare species such as circulating tumor cells could be captured using immunoaffinity based assays on functionalized slides.³² Additional downstream analysis of such cells, for gene expression or therapy response,²⁹ could then be performed using the diffusive filter described herein. On a more general level, when analyzing mixtures of immobilized species, a solvent composition can be tuned to selectively retrieve a particular species of interest in a user-defined manner. Finally, an addition of more apertures to increase the number of parallel streams has potential utility for flow fractionation applications, and since our diffusive filter does not incorporate any membranes, it is free from common problems, such as membrane fouling and membrane clogging. The use of silicon wafers to fabricate these filters is further advantageous due to reliable and standard manufacturing methods and solvent resistance of silicon as compared to soft lithography-based devices.³³ To conclude, we have presented a novel method for the local retrieval of surface bound species and their rapid in-line separation using an open space microfluidic device.

ASSOCIATED CONTENT

Supporting Information

The Supporting Information is available free of charge at <https://pubs.acs.org/doi/10.1021/acs.analchem.0c02176>.

SI: Interdependence of separation distance, diffusivity, and flow velocity; experimental setup describing various components; manufacturing process of horizontal microfluidic device; simulation of flow profile in the absence of stabilization flows; derivation of governing equation for a T-sensor; Geometry calculation for hMFP – separation of beads and dye; separation efficiency for multiple experimental runs; diffusivity measurement in different experimental runs (PDF)

Surface retrieval and separation of RBCs (AVI)

Video explanation of the work (MP4)

AUTHOR INFORMATION

Corresponding Authors

Andrew J. deMello – Institute for Chemical and Bioengineering, Dept. of Chemistry and Applied Biosciences, Eidgenössische Technische Hochschule (ETH-Zürich), 8093 Zürich, Switzerland; orcid.org/0000-0003-1943-1356; Email: andrew.demello@chem.ethz.ch

Govind V. Kaigala – IBM Research Europe, CH-8803 Rüschlikon, Switzerland; orcid.org/0000-0003-1145-7287; Email: gov@zurich.ibm.com

Authors

Prerit Mathur – IBM Research Europe, CH-8803 Rüschlikon, Switzerland; Institute for Chemical and Bioengineering, Dept. of Chemistry and Applied Biosciences, Eidgenössische Technische Hochschule (ETH-Zürich), 8093 Zürich, Switzerland

Anna Fomitcheva Khartchenko – IBM Research Europe, CH-8803 Rüschlikon, Switzerland; Institute for Chemical and Bioengineering, Dept. of Chemistry and Applied Biosciences, Eidgenössische Technische Hochschule (ETH-Zürich), 8093 Zürich, Switzerland

Complete contact information is available at:

<https://pubs.acs.org/10.1021/acs.analchem.0c02176>

Author Contributions

P.M., A.F.K., A.M. and G.V.K. conceived the presented idea. P.M. and A.F.K. designed the experiments. P.M. performed the experiments. All authors contributed to writing the manuscript.

Notes

The authors declare no competing financial interest.

ACKNOWLEDGMENTS

We gratefully acknowledge funding from the ERC-PoC grant CellProbe (842790). We would like to acknowledge Prof. Moran Bercovici (Technion), Dr. Aditya Kashyap, Dr. Robert Lovchik, Dr. Iago Pereiro, Hanut Vemulapalli, and Dr. Stavros Stavrakis (ETH-Z) for helpful discussions. We would also like to thank Dr. Federico Paratore for assistance with the design and fabrication of the MFP heads. Ute Drechsler and Stefan Gamper are acknowledged for their help in manufacturing and fabrication. P.M., A.F.K., and G.V.K. are grateful to Dr. Emmanuel Delamarche and Dr. Heike Riel for their continued support.

REFERENCES

- (1) Gossett, D. R.; Weaver, W. M.; Mach, A. J.; Hur, S. C.; Tse, H. T. K.; Lee, W.; Amini, H.; Di Carlo, D. *Analytical and Bioanalytical Chemistry* **2010**, 3249–3267, DOI: 10.1007/s00216-010-3721-9.
- (2) Giddings, J. C.; Yang, F. J. F.; Myers, M. N. *Science* **1976**, 193 (4259), 1244–1245.

- (3) Dupont, A. L.; Mortha, G. *J. Chromatogr. A* **2004**, 1026 (1–2), 129–141.
- (4) Huang, L. R.; Cox, E. C.; Austin, R. H.; Sturm, J. C. *Science* **2004**, 304 (5673), 987–990.
- (5) Blom, M. T.; Chmela, E.; Oosterbroek, R. E.; Tijssen, R.; Van Den Berg, A. *Anal. Chem.* **2003**, 75 (24), 6761–6768.
- (6) Tian, F.; Zhang, W.; Cai, L.; Li, S.; Hu, G.; Cong, Y.; Liu, C.; Li, T.; Sun, J. *Lab Chip* **2017**, 17 (18), 3078–3085.
- (7) Fischer, C. H.; Giersig, M. *J. Chromatogr. A* **1994**, 688 (1–2), 97–105.
- (8) Bacheva, V.; Paratore, F.; Rubin, S.; Kaigala, G. V.; Bercovici, M. *Angew. Chem.* **2020**, DOI: 10.1002/ange.201916699.
- (9) Brody, J. P.; Yager, P. *Sens. Actuators, A* **1997**, 58 (1), 13–18.
- (10) Kamholz, A. E.; Schilling, E. A.; Yager, P. *Biophys. J.* **2001**, 80 (4), 1967–1972.
- (11) Osborn, J. L.; Lutz, B.; Fu, E.; Kauffman, P.; Stevens, D. Y.; Yager, P. *Lab Chip* **2010**, 10 (20), 2659–2665.
- (12) Weigl, B. H.; Kriebel, J.; Mayes, K. J.; Bui, T.; Yager, P. *Microchim. Acta* **1999**, 131 (1–2), 75–83.
- (13) Helton, K. L.; Nelson, K. E.; Fu, E.; Yager, P. *Lab Chip* **2008**, 8 (11), 1847–1851.
- (14) Navvab Kashani, M.; Kriel, F. H.; Binder, C.; Priest, C. *Microfluid. Nanofluid.* **2020**, 24 (3), 1–10.
- (15) Birmingham, K. G.; O'Melia, M. J.; Ban, D.; Mouw, J.; Edwards, E. E.; Marcus, A. I.; McDonald, J.; Thomas, S. N. *Adv. Biosyst.* **2019**, 3, 1800328.
- (16) Gavutis, M.; Navikas, V.; Rakickas, T.; Vaitekoniš, Š.; Valiokas, R. *J. Micromech. Microeng.* **2016**, 26 (2), 025016.
- (17) Chen, C. Y.; Li, H. H.; Chu, H. Y.; Wang, C. M.; Chang, C. W.; Lin, L. E.; Hsu, C. C.; Liao, W. S. *ACS Appl. Mater. Interfaces* **2018**, 10 (48), 41814–41823.
- (18) Autebert, J.; Kashyap, A.; Lovchik, R. D.; Delamarche, E.; Kaigala, G. V. *Langmuir* **2014**, 30 (12), 3640–3645.
- (19) Kashyap, A.; Autebert, J.; Delamarche, E.; Kaigala, G. V. *Sci. Rep.* **2016**, 6 (1), 1–10.
- (20) Kulak, N. A.; Pichler, G.; Paron, I.; Nagaraj, N.; Mann, M. *Nat. Methods* **2014**, 11 (3), 319–324.
- (21) Bruus, H. *Theoretical Microfluidics*; Oxford University Press: Cambridge, 2007; Vol. 18. DOI: 10.1017/CBO9781107415324.004.
- (22) Tabeling, P. *Introduction to Microfluidics*; Oxford University Press, 2005.
- (23) Petrášek, Z.; Schwille, P. *Biophys. J.* **2008**, 94 (4), 1437–1448.
- (24) Pereiro, I.; Cors, J. F.; Pané, S.; Nelson, B. J.; Kaigala, G. V. *Chem. Soc. Rev.* **2019**, 48 (5), 1236–1254.
- (25) Robb, J. S.; Robb, A. G.; Robson, D. C. Red Blood Cell Detection. EP3108247A1, 2014.
- (26) Campbell, C. J.; O'Looney, N.; Chong Kwan, M.; Robb, J. S.; Ross, A. J.; Beattie, J. S.; Petrik, J.; Ghazal, P. *Anal. Chem.* **2006**, 78 (6), 1930–1938.
- (27) Cita, K. C.; Brureau, L.; Lemonne, N.; Billaud, M.; Connes, P.; Ferdinand, S.; Tressières, B.; Tarer, V.; Etienne-Julan, M.; Blanchet, P.; Elion, J.; Romana, M. *PLoS One* **2016**, 11 (5), e0154866.
- (28) Shevkoplyas, S. S.; Yoshida, T.; Gifford, S. C.; Bitsensky, M. W. *Lab Chip* **2006**, 6 (7), 914–920.
- (29) Sharma, S.; Zhuang, R.; Long, M.; Pavlovic, M.; Kang, Y.; Ilyas, A.; Asghar, W. *Biotechnology Advances* **2018**, 1063–1078, DOI: 10.1016/j.biotechadv.2018.03.007.
- (30) Yi, X.; Liu, M.; Luo, Q.; Zhuo, H.; Cao, H.; Wang, J.; Han, Y. *FEBS Open Bio* **2017**, 7 (4), 485–494.
- (31) Lee, S. S.; Ahn, K. H.; Lee, S. J.; Sun, K.; Goedhart, P. T.; Hardeman, M. R. *Korea-Australia Rheol. J.* **2004**, 16 (3), 141–146.
- (32) Bankó, P.; Lee, S. Y.; Nagygyörgy, V.; Zrínyi, M.; Chae, C. H.; Cho, D. H.; Telekes, A. *Journal of Hematology and Oncology* **2019**, DOI: 10.1186/s13045-019-0735-4.
- (33) Yadavali, S.; Lee, D.; Issadore, D. *Sci. Rep.* **2019**, 9 (1), 1–10.